

## UPDATED IMPEDANCE ESTIMATE OF THE PEP-II RF CAVITY\*

R.A. Rimmer, J. Byrd, M. Irwin, D.A. Goldberg,  
Lawrence Berkeley National Laboratory, 1 Cyclotron Road, Berkeley, CA 94720, USA

and

Stanford Linear Accelerator Center, Stanford, CA 94309, USA

### Abstract

This paper presents an updated estimate of the higher-order mode impedance spectrum of the RF cavities for the PEP-II B-factory. The cavity is designed for continuous operation at 476 MHz with up to 150 kW wall dissipation and heavy beam loading. To reduce the growth rates of coupled-bunch instabilities the cavity higher-order modes are damped by three rectangular waveguides and broad-band loads. The results of detailed measurements on the first high-power cavity with all absorbers in place are presented and the damping effect due to the high-power coupler is discussed. Results are compared with earlier measurements of a cold-test model. Implications for the design of the broad-band bunch-by-bunch feedback systems and high-power HOM loads are discussed.

*Contributed to the 5th European Particle Accelerator Conference (EPAC 96)  
Sitges, Barcelona, Spain  
June 10-14, 1996*



slw649

---

\* Work supported by Department of Energy contract DE-AC03-76SF00515 (SLAC), DE-AC03-76SF00098 (LBNL).

# UPDATED IMPEDANCE ESTIMATE OF THE PEP-II RF CAVITY\*

R.A. Rimmer, J. Byrd, M. Irwin, D.A. Goldberg, LBNL, Berkeley, CA, USA

## Abstract

This paper presents an updated estimate of the higher-order mode impedance spectrum of the RF cavities for the PEP-II B-factory. The cavity is designed for continuous operation at 476 MHz with up to 150 kW wall dissipation and heavy beam loading. To reduce the growth rates of coupled-bunch instabilities the cavity higher-order modes are damped by three rectangular waveguides and broad-band loads. The results of detailed measurements on the first high-power cavity with all absorbers in place are presented and the damping effect due to the high-power coupler is discussed. Results are compared with earlier measurements of a cold-test model. Implications for the design of the broad-band bunch-by-bunch feedback systems and high-power HOM loads are discussed.

## 1 INTRODUCTION

The PEP-II B-factory is a machine designed to achieve a high integrated luminosity through the use of many bunches and high average current in both rings. The control of coupled-bunch instabilities is therefore of great importance and a large fraction of the impedance budget of the machine comes from the higher-order modes (HOMs) of the RF cavities. The method of damping these HOMs and estimates of the residual impedance have been previously reported [1,2], based on measurements of a cold-test model of the PEP-II cavity design. This paper reports recent measurements of the first high-power cavity, which differs from the cold-test model in having a large iris coupler and in other details. Techniques developed while analyzing the data from the cold-test cavity [3,4], were applied to measurements of the frequency spectrum and mode field profiles in the high-power cavity. In particular the ability to extract the loaded Q's of multiple overlapping resonances by curve fitting and to take automated bead-pull field mapping data on and off the beam axis were essential. The results of the measurements including frequencies, loaded Q's and mode impedances are summarized in tables 1 and 2

## 2 HIGH-POWER CAVITY RESULTS

The main difference between the cold-test model and the high-power cavity is the addition of the iris coupling port in the horizontal plane. The nose-cone gap is also slightly different to compensate for the added volume of the coupler and because of some weld shrinkage during final assembly of the cavity, (hence the measured

\*This work was supported by the U.S. Department of Energy under contract DE-AC03-76SF00098 .

frequency of the fundamental mode in table 1 is slightly low at 475 MHz, this was corrected using a fixed tuner for high-power testing). The calculated frequencies and R/Q's in tables 1 and 2 are from a 2D model with the same nose-cone spacing as the high-power cavity and are used only as a guide to the expected frequency and strength of the modes.

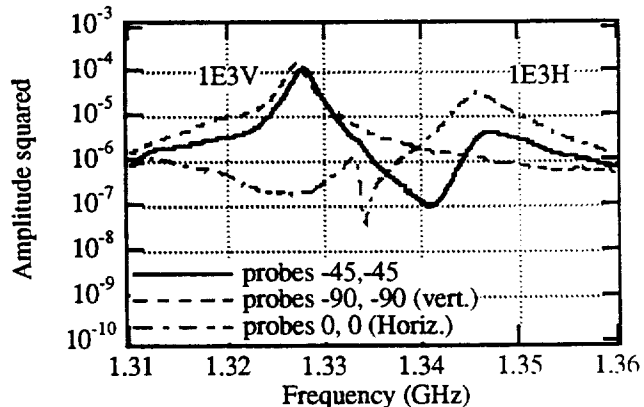


Figure 1. Splitting of 1-E-3 dipole mode in spectrum.

The high-power cavity was assembled with a cold-test model of the coupler, including a window and ferrite HOM load, and with cold-test loads on the 3 cavity HOM ports. The feeder waveguide was terminated in a sheet of resistive absorber, which proved a good match for the higher frequencies.

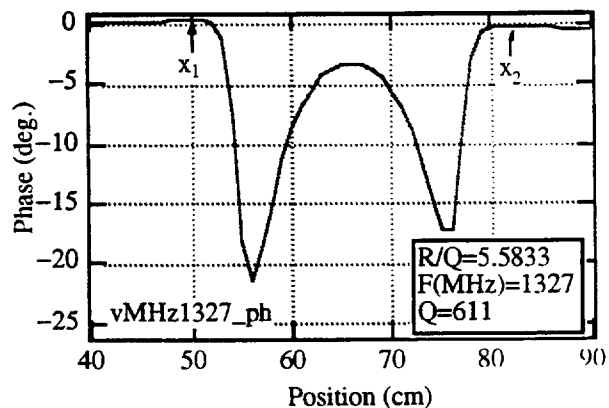


Figure 2. Bead-pull data of 1-E-3V mode 4 cm off axis.

The cavity was excited by small electric field probes in the beam pipes and the frequency response was recorded with 100 kHz resolution from 0.4 to 2.4 GHz (with some spectra up to 4.9 GHz), with the probes in horizontal, vertical, 45° and staggered (90° apart) orientations. This allowed for the identification of modes from their orientation in the cavity, and independent measurements of the Q's and impedances of both versions of the dipole modes, e.g. 1-E-3V and 1-E-3H, see figures 1 and 2.

Table 1. Impedance of longitudinal modes estimated from calculated and measured R/Q's and measured (fitted) Q's.

mode <sup>‡</sup>	f calc.2D (GHz)	R/Q calc.2D (Ω)	f meas. (GHz)	R/Q meas. (Ω)	Q meas. (fitted)	Rs (kΩ) (calc R/Q)	Rs (kΩ) (meas R/Q)
0-E-1	0.480	116.358	0.475	117.3	14218	1654	1668
0-M-1	0.756	39.903	0.758	44.6	18*	0.72	0.81
0-E-2	1.003	0.360	1.009	0.43	128	0.046	0.055
new			1.283	6.70	259	-	1.74
0-M-2	1.288	7.000	1.295	10.3	222	1.56	2.29
0-E-3	1.289	7.062	n.v.	n.v.	30*	0.21	n.v.
0-E-4	1.584	3.870	1.595	2.43	300	1.16	0.73
0-M-3	1.711	5.324	1.710	0.44	320	1.70	0.14
0-E-5	1.818	0.029	1.820	0.13	543*	0.016	0.070
0-M-4	1.894	0.848	1.898	0.17	2588	2.19	0.44
0-E-6	2.112	5.171	2.121	1.82	338	1.75	0.62
0-M-5	2.162	0.019	2.160	0.053	119*	0.002	0.006
0-E-7	2.255	1.009	2.265	0.064	1975*	1.99	0.13
0-E-8	2.359	0.141	2.344	n.m.	693*	0.10	n.m.

<sup>‡</sup>E = electric field, M = magnetic field boundary condition at cavity center. \* Approx. fit or worst-case estimate  
n.v. = mode not visible after damping. n.m. = mode not measured

Table 2. Transverse impedance of dipole modes estimated from calculated and measured R/Q's and measured Q's.

mode <sup>‡</sup>	f calc.2D (GHz)	R/Q@4.76cm (Ω) calc.2D	f meas. (GHz) meas.	R/Q(Ω)@4cm bead-pull	Q meas. (fitted)	R <sub>⊥</sub> calc.† (kΩ/m)	R <sub>⊥</sub> meas.† (kΩ/m)
1-M-1 H	0.686	0.089	n.v.	n.v.	n.v.	n.v.	n.v.
1-M-1 V	0.686	0.089	n.v.	n.v.	n.v.	n.v.	n.v.
1-E-1 H	0.796	11.529	n.v.	n.v.	n.v.	n.v.	n.v.
1-E-1 V	0.796	11.529	0.792	9.69	115*	34.9	42.0
1-M-2 V	1.068	32.042	1.063	50.4	27	16.9	38.0
1-M-2 H	1.068	32.042	1.068	n.m.	25	15.9	n.m.
1-E-2 H	1.127	0.161	1.120	n.v.	31*	0.092	n.v.
1-E-2 V	1.127	0.161	1.133	1.29	54*	0.16	1.82
1-M-3 V	1.212	0.675	1.202	0.56	871	10.1	12.2
1-M-3 H	1.212	0.675	1.205	0.90	723	8.44	16.1
1-E-3 H	1.333	6.065	1.346	3.96	323	31.2	28.3
1-E-3 V	1.333	6.065	1.327	5.58	611	58.3	76.7
1-M-4 V	1.413	9.421	1.420	5.31	1138	160.7	126.9
1-M-4 H	1.413	9.421	1.425	3.30	414	58.7	28.6
1-E-4 H	1.542	1.997	1.540	1.57	73*	1.99	2.22
1-E-4 V	1.542	1.997	1.542	0.50	92*	2.51	0.89
1-E-5 V	1.603	4.107	1.595	0.51	145*	7.78	1.39
1-E-5 H	1.603	4.107	1.599	0.29	146*	7.83	0.80
1-E-6 H	1.668	15.477	1.670	3.61	377	73.8	24.3
1-E-6 V	1.668	15.477	1.676	4.63	783	153.8	64.5
1-M-5 V	1.738	0.032	1.723	n.v.	446*	0.18	n.v.
1-M-5 H	1.738	0.032	1.727	n.v.	320*	0.13	n.v.
1-M-6 V	1.766	0.154	1.749	0.10	1317	2.41	2.31
1-M-6 H	1.766	0.154	1.756	0.12	2664	4.90	5.35

<sup>‡</sup>H = horizontal, V = vertical orientation of mode. \* Approx. fit or worst-case estimate. †R<sub>⊥</sub> = R/(Qkr<sup>2</sup>)\*Q<sub>L</sub>  
n.v. = mode not visible after damping. n.m. = mode not measured

The two orientations of the dipole modes appear with different frequencies and Q's because of the breaking of the azimuthal symmetry, chiefly by the iris coupler in the horizontal plane. In the low-power cavity the dipole modes were only weakly perturbed and the frequencies and Q's of the quasi-degenerate modes were very similar.

The spectra were recorded by a computer which controlled the network analyzer and also ran the automated bead-puller. The spectra were then recalled and the Q's of the peaks extracted using routines that enabled the fitting of multiple overlapping Lorentzian functions to the data. This was essential to the extraction of Q's from weak modes in the presence of strong peaks and of groups of modes that were close together in frequency. The measured frequencies and loaded Q's of the monopole and dipole modes are presented in tables 1 and 2.

Once the modes were identified the bead-puller was used to measure their field profiles and the data were processed to estimate the longitudinal or transverse beam impedances. Figure 2 shows the phase shift perturbation of the 1-E-3V dipole mode by a needle pulled through the cavity 4 cm above the beam axis. This is used to calculate the longitudinal impedance at that radius and hence the transverse impedance of the mode. The last columns in tables 1 and 2 show the longitudinal or transverse impedances of the modes estimated from the measured R/Q's and loaded Q's.

### 3 EFFECT OF THE COUPLER

The effect of adding the coupler is to separate the horizontal and vertical versions of the dipole modes in frequency, and to provide extra damping to those modes that have magnetic field at the iris. Since the iris is offset slightly from the equator it may couple to both M- and E-type modes and in many cases, such as 1-M-4H and 1-E-6H, useful additional damping may be obtained. This explains the lower Q's of the horizontal versions of the modes. The coupler load, which is located in a short waveguide off of the coupler bend, also helps some of the monopole modes. However because the coupling to this load is less effective at low frequencies there is some extra structure in the spectrum between 0.7 GHz and about 1.3 GHz from resonances in the coupler box. All of these new peaks were measured with the bead-puller and only the peak at 1.283 GHz was found to have any significant impedance. This appears to have a field profile on axis similar to the 0-M-2 mode at 1.295 GHz and is probably the result of coupling between this mode and a box resonance at about the same frequency.

### 4 EFFECT OF REAL LOADS

The cold-test loads used on the HOM ports of the high-power cavity were the same as previously used on the low-power model, which allows comparison of the results from the two experiments. The real high-power loads behave similarly to the cold-test loads at high

frequencies, but below about 1 GHz they are less well matched, with a VSWR rising to approximately 2:1 at 0.7 GHz. Cold-test mock-ups of the real load geometry were applied to the low-power test cavity to see the effect on the lowest modes. This introduced some new structure in the spectrum between about 0.6 and 1 GHz, which has the effect of enhancing or reducing (depending on the phase of the reflection from the loads), the effective impedance seen by the beam. This modulation does not appear to increase the effective impedance by more than a small factor, so any resulting instability growth rates are expected to be safely within the capabilities of the bunch-by-bunch feedback systems.

## 5 CONCLUSIONS

The HOM impedances for the high-power cavity are as good as or better than those observed in the cold-test model, mainly due to the symmetry-breaking perturbation and additional damping of the coupler and its ferrite load. Although resonances in the coupler at low frequency show up in the cavity spectrum most of the new peaks do not have any significant impedance.

Reflections from the cavity HOM loads at low frequency may also modify the driving impedance for coupled-bunch instabilities and/or power extracted from the beam by a small factor.

Because the impedances of the cavity modes appear to be generally the same as or lower than previous estimates the growth rates of coupled-bunch instabilities are expected to be within the capabilities of the bunch-by-bunch feedback systems. Growth rates of higher-order transverse coupled-bunch instabilities such as the  $m=1$  modes, which are not addressed by the feedback systems, are expected to be below the natural damping rates of both rings, however further damping can be applied to specific HOMs if required.

## REFERENCES

- [1] "RF Cavity Development for the PEP-II B Factory", R.A. Rimmer, Proc. Int. Workshop on B-Factories, BFWS92, KEK, Japan, Nov. 17-20, 1992, LBL-33360, and PEP-II EE Note 3-94.
- [2] "Measurements of Higher-Order Mode Damping in the PEP-II Low-Power Test Cavity", R.A. Rimmer, D.A. Goldberg, Proc. P.A.C., Washington D.C., May 17-20, 1993, LBL-33312.
- [3] "Measurement and Analysis of Higher-Order Mode (HOM) Damping in B-Factor R-F cavities", D.A. Goldberg et. al., Proc. PAC95, Dallas, Texas, May 1-5 1995.
- [4] "Automated Bead-Positioning System for Measuring Impedances of R-F Cavity Modes", D.A. Goldberg, R.A. Rimmer, Proc. P.A.C., Washington D.C., May 17-20, 1993, LBL-33280.